Different Approaches to Grounding Resistance Calculation for Thin Wire Structures at Low Frequency Energization

E. Faleiro, G. Asensio, G. Denche, D. García , J. Moreno

***Abstract*— The present paper deals with the calculation of grounding resistance of an electrode composed of thin wires, that we consider here as perfect electric conductors (PEC) e.g. with null internal resistance, when buried in a soil of uniform resistivity. The potential profile at the ground surface is also calculated when the electrode is energized with low frequency current. The classic treatment by using leakage currents, called Charge Simulated Method (CSM), is compared with that using a set of steady currents along the axis of the wires, here called the Longitudinal Currents Method (LCM), to solve the Maxwell equations. The method of moments is applied to obtain a numerical approximation of the solution by using rectangular basis functions. Both methods are applied to two types of electrodes and the results are also compared with those obtained using a thirth approach, the Average Potential Method (APM), later described in the text. From the analysis performed, we can estimate a value of the error in the determination of grounding resistance as a function of the number of segments in which the electrodes are divided.**

***Index Term*— Low frequency current energization, electromagnetic analysis, grounding grids, grounding resistance, method of moments.**

I. Introduction

The problem of grounding grid analysis techniques with low frequency current energization has been widely treated by several authors along decades [1]-[9]. The methods used for the analysis of grounding grids could be classified according to the type of current source energization applied to the grounding grid conductors. According to those criteria, one can distinguish two types of grounding grid current energization: the low frequency current energization which is also sometimes known by direct current regime, and the high frequency energization. In the latter, the analysis of the grounding grid transients is carried out. In this paper, the focus is on the first type.

According to the theoretical scheme used to solve the problem, one can make a clear distinction between a circuit approach, an electromagnetic theory approach and a hybrid approach in order to calculate grounding resistance as well as step and touch voltages at ground level. The circuit approach is said to be fast and relatively easy to understand, but at the same time the least accurate one. The electromagnetic approach is believed to be the most accurate one, due to the least amount of approximations, but at the same time numerically intensive and relatively difficult to understand. The main difficulty in applying the electromagnetic approach stems from the complex mathematical apparatus, which transforms Maxwell equations into a system of algebraic equations, and its associated numerical implementation. Here one can distinguish between a finite element approach, a boundary element approach and an approach according to the method of moments [12]-[15]. The hybrid approach is a mixture between the two above-mentioned approaches and can vary in complexity as well as in accuracy.

Since the analytical solutions are available only for very few cases, numerical methods were firstly applied to the solution of the so-called equipotential grounding grids, buried in homogeneous, two-layer or multi-layer horizontally stratified earth [10]-[11], and energized with a low frequency current. Due to this current energization, only self and mutual leakage conductance of grounding grid elements had to be considered. Conductors were treated as infinitely conductive or PEC. One of the most prominent of the methods applied in this field is the CSM or Charge Simulated Method [4],[6],[9] in which a set of variable leakage current densities needs to be calculated in order the electrode to be equipotential. The method is simple though, as will be seen later, is very sensitive to the numerical scheme used in your application.

Faced with this method which uses only leakage currents to ground, we will use a low frequency approach of the Electric Field Integral Equation scheme (EFIE) [17], which uses only longitudinal currents along the axis of the wires. This method is called here Longitudinal Currents Method or LCM. As in the CSM method, the solution is found numerically which is also sensitive to the numerical scheme used. The LCM method is much more complex and computationally expensive than the CSM so almost all low frequency applications are treated with the CSM method. However, as will be seen later, both methods complement each other and provide valuable information about errors in the calculation of relevant electrical quantities.

There is to be mentioned as well the so-called APM or Average Potential Method [2],[3] in which every portion of the electrode delivers an uniform and constant current density to the surroundings. The potentials on the electrodes are calculated by averaging the local potentials. Both CSM and APM methods make use of a leakage currents scheme that produces the potential profile around.

The authors are with the Escuela Técnica Superior de Ingeniería y Diseño Industrial (ETSIDI) at Universidad Politécnica de Madrid (UPM), Dept. of Applied Physics, Dept. of Applied Mathematics and Dept. of Electrical Engineering, Ronda de Valencia 3, 20012-Madrid (corresponding author E. Faleiro, e-mail: eduardo.faleiro@upm.es).

In this paper we will use the electromagnetic approach to implement a computer code to numerically solve the problem of finding the response of a thin wire structure to a low frequency excitation. The two complementary methods CSM and LCM will be used for calculating the grounding resistance of a thin wire structure. The APM method were used as a test. The CSM method is well described in the references and we will not give any details about their numerical implementation. On the contrary, as to due to its complexity, we will focus on the theoretical foundations of LCM method indicating some of the most important steps to get to a numerical implementation of it. So a system of currents along the conductor axis, as sources for electromagnetic fields, will be used and a methodology similar to that applied for the transient analysis of grounding grids is applied [17],[18].

The method of moments is employed to find the numerical distribution of longitudinal currents in order to calculate the grounding resistance and the absolute potential profile at the earth surface. A careful analysis of the grounding resistance dependence with the numerical scheme is done showing that the CSM and LCM methods have a close dependence on the segmentation of the electrodes. Finally, by using several geometric shapes for electrodes, the grounding resistance and the potential profile at the earth surface are obtained by the CSM and LCM methods and compared with those calculated by the APM method.

II. THEORETICAL FOUNDATIONS

As a start, a PEC thin wire buried in a semi-infinite medium of conductivity sigma and powered by a low frequency electric current injected through any point on its surface or by its ends is used. The electric potential profile in the surrounding environment created by the leakage current to the ground can be found by solving Maxwell's equations. For a free charge density ρ_l and free current density, $\vec{J}_l = \vec{J}_c + \vec{J}_s$ where $\vec{J}_c$ is the conduction current density which according to the Ohm's law, $\vec{J}_c = \sigma\vec{E}$, and it is assumed that the electrical conductivity σ is a constant. Now, it is supposed that the current density $\vec{J}_l$ is stationary and the continuity equation $\vec{\nabla}\vec{J}_l = 0$ is verified, which means that,

$$\sigma\vec{\nabla}\vec{E} + \vec{\nabla}\vec{J}_s = 0. \tag{1}$$

By using Maxwell's equations, it can be found that

$$\vec{\nabla}\vec{J}_s = -\frac{\sigma}{\varepsilon}\rho_l, \tag{2}$$

$\vec{J}_s$ being a current flowing along the wire, and $\vec{J}_c$ being a current flowing to the outside environment, that is, the leakage current.

For a low frequency problem, electromagnetic potentials $\vec{A}$ and ϕ satisfy the equations,

$$\vec{\nabla}^2\phi = -\frac{\rho_l}{\varepsilon} \tag{3}$$

$$\vec{\nabla}^2\vec{A} = -\mu\vec{J}_s. \tag{4}$$

Here, the so-called thin wire approach [12], which states that charges and currents in a thin wire electrode can be replaced by charges and currents along its axis which will produce the same electromagnetic fields in both its surface and in the external environment, is used. Thus, the solution to (3) and (4) for a curved conductor wire is

$$\phi(\vec{r}) = \int_{L'} \frac{\rho_l(s')}{4\pi\varepsilon} \cdot \frac{ds'}{|\vec{r} - \vec{r}'(s')|} \tag{5}$$

$$\vec{A}(\vec{r}) = \int_{L'} \frac{\vec{I}_s(s')}{4\pi\varepsilon} \cdot \frac{ds'}{|\vec{r} - \vec{r}'(s')|} \tag{6}$$

where $\rho_l(s')$ is the free electric charge density along the wire axis and $I_s(s')$ is the current flowing through the wire axis. Here, s' is a variable used to locate points on the wire axis, whose value is the distance from one end of the wire (Fig. 1). These charges and currents have to be previously calculated knowing the boundary conditions as well as how the electrode is energized.

A scheme leading to a satisfactory solution is obtained from the electric field generated by the buried structure $\vec{E} = -\vec{\nabla}\phi$ where the potential is to be calculated from (2) and (5) which results

$$\phi(\vec{r}) = \int_{L'} \frac{-\vec{\nabla}'\vec{J}_s(\vec{r}'(s'))}{4\pi\sigma} \cdot \frac{ds'}{|\vec{r} - \vec{r}'(s')|}. \tag{7}$$

Note that the spatial variation of the longitudinal currents along the wire axis, provides the leakage currents to the

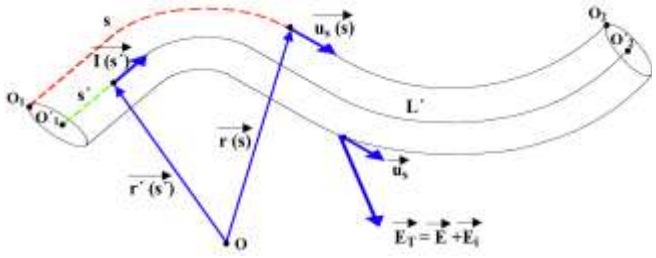

Fig. 1. A conductive curved thin wire where some of the variables used in the text are shown. Longitudinal current $I_s(s')$ has been drawn at a specific point s' of the wire axis. The total electric field is also shown in the same figure with the tangent vector $\vec{u}_s$ along which the total electric field has to be projected.

outside environment. Using the continuity of the tangential component of the total electric field at the surface of the conductor (Fig. 1), it holds that

$$(\vec{E}_i + \vec{E}) \cdot \vec{u}_s = 0. \tag{8}$$

This expression is valid for a PEC. Otherwise, the second member of (8) needs to be replaced by a quantity proportional

to the conductor impedance. The electric field $\vec{E}_i$ is the impressed field and will generate induced fields $\vec{E}$ and $\vec{B}$, while the vector $\vec{u}_s = \frac{d\vec{r}(s)}{ds}$ is a unitary tangent vector at the electrode surface (Fig. 1). For a PEC, it holds that

$$\vec{E}_i \cdot \vec{u}_s = -\vec{E} \cdot \vec{u}_s = \vec{u}_s \cdot \vec{\nabla}\phi. \tag{9}$$

Now, the potential expressed in terms of the longitudinal currents is introduced. To do this an integration by parts is done,

$$\vec{E}_i \cdot \vec{u}_s = \vec{u}_s \cdot \vec{\nabla}\phi = \vec{u}_s \cdot \vec{\nabla}\int_{L'} \frac{-\vec{\nabla}'\vec{J}_s(\vec{r}'(s'))}{4\pi\sigma} \cdot \frac{ds'}{|\vec{r} - \vec{r}'(s')|} =$$

$$= -\frac{1}{\sigma}\vec{u}_s \cdot \vec{\nabla}\int_{L'} \frac{\partial I(s')}{\partial s'} G(s,s')ds' =$$

$$-\frac{1}{\sigma}\frac{\partial}{\partial s}\int_{L'} [\frac{\partial}{\partial s'}(I(s')G(s,s')) - I(s')\frac{\partial}{\partial s'}G(s,s')]ds' =$$

$$= -\frac{1}{\sigma}\frac{\partial}{\partial s}Cont(s) + \frac{1}{\sigma}\frac{\partial}{\partial s}\int_{L'} I(s')\frac{\partial}{\partial s'}G(s,s')ds' \tag{10}$$

by using the identity $\vec{u}_s \cdot \vec{\nabla} \equiv \frac{\partial}{\partial s}$. Moreover, the kernel

$$G(s,s') = \frac{1}{4\pi\sigma|\vec{r}(s) - \vec{r}'(s')|} \tag{11}$$

has been introduced where s and s' variables refer to the positions of the field points and source points respectively. For longitudinal currents along the wire axis, the next relationship has been taken into account,

$$-\vec{\nabla}'\vec{J}_s(\vec{r}'(s')) \equiv -\frac{\partial I(s')}{\partial s'} \tag{12}$$

In expression (10), $Cont(s)$ takes into account the boundary conditions at the ends of the conductor,

$$Cont(s) = (I(s')G(s,s'))_{s'=i}^{s'=d} = I(d)G(s,d) - I(i)G(s,i) \tag{13}$$

$I(i)$ and $I(d)$ being the currents in the wire ends, which correspond to the current value for $s' = 0$ (point O'$_1$ in Fig. 1) and $s' = L'$ (point O'$_2$ in Fig. 1). Those currents will be zero unless a driving current is injected or released through these ends. If the conductor is a closed wire, $Cont(s)$ equals zero. Note that the expression (10) contains only the longitudinal currents as unknowns of the problem, so it can be considered as an integral Fredholm equation of the first type.

III. NUMERICAL SOLUTION USING THE METHOD OF MOMENTS

The method of moments is a numerical procedure that allows obtaining a solution to equation (10) by reducing the integral equation to a matrix equation [12]. To do this, the overall curved wire of length L, is divided into N small sized line segments $\Delta s' = L/N$. A selected set of known functions is chosen to build a linear approximation to the unknown function $I(s')$,

$$I(s') = \sum_{n=1}^{N} I_n \cdot u_n(s') \tag{14}$$

as an example, the unit step function can be chosen for $u_n(s')$,

$$u_n(s') = 1 \ldots if \ldots (n-1)\Delta s' < s' < n\Delta s'$$
$$u_n(s') = 0 \ldots otherwise \tag{15}$$

Note that this is a staircase-like approximation to the function $I(s')$, for which $I(s'=0) = I_0$, while $I(s'=L') = I_{N+1}$, I_0 and I_{N+1} being the currents flowing to the left and right of the wire, respectively, according with the step functions in (14) and (15).

The choice of these functions u_n is made for simplicity, but they are neither the only possible nor the best numerical results to be provided. In this paper the functions (14) were chosen because of their simplicity at the risk of losing some accuracy in the final results [13],[14].

By renaming $E_i(s) = \vec{E}_i \cdot \vec{u}_s$, and taking into account (13) and (14), it follows that

$$E_i(s) = -\frac{1}{\sigma}[I_{N+1}\frac{G(s+\frac{\Delta s}{2},N) - G(s-\frac{\Delta s}{2},N)}{\Delta s} -$$
$$- I_0\frac{G(s+\frac{\Delta s}{2},0) - G(s-\frac{\Delta s}{2},0)}{\Delta s}] + \frac{1}{\sigma}\frac{\partial}{\partial s}\sum_{n=1}^{N} I_n[G(s,n) - G(s,n-1)] \tag{17}$$

where the notation is simplified by writing $G(s,n)$ instead of $G(s,n\Delta s')$.

This expression is valid at any point s on the electrode surface. Finally, a set of N weighting functions are being used such as the Dirac delta function,

$$w_m(s) = \delta(s - s_m) \tag{18}$$

where the points s_m are on the electrode surface and are chosen arbitrarily. It is usual that they are aligned perpendicular to the midpoints of the segments $\Delta s'$ on the axis wire (Fig. 2).

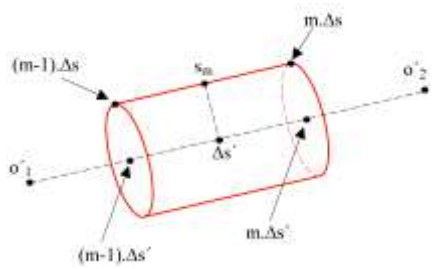

Fig 2. Detailed representation of a conductive wire segment with some of the variables used in the text.

With this choice of weighting functions for each point s_m, the expression (17) results,

$$E_i(s_m)\cdot\Delta s = -\frac{1}{\sigma}[I_{N+1}(G(m,N)-G(m-1,N))-I_0(G(m,0)-G(m-1,0))]+ \quad (19)$$
$$+\frac{1}{\sigma}\sum_{n=1}^{N} I_n(G(m,n)-G(m-1,n)-G(m,n-1)-G(m-1,n-1)),$$

where the notation is simplified as before by writing $G(m,n)$ instead of $G(m\Delta s, n\Delta s')$.

In practice, for a wire to which a low frequency current I_{in} is applied by one of its free ends, whereas another direct current I_{out} is delivered to the external environment by the other free end, the equation (18) applied to the N points s_m constitutes a non-homogeneous linear system of N+2 equations,

$$\begin{pmatrix} 1 & 0 & 0 & \dots & 0 \\ Z_{10} & Z_{11} & Z_{12} & \dots & Z_{1,N+1} \\ Z_{20} & Z_{21} & Z_{22} & \dots & Z_{2,N+1} \\ \dots & \dots & \dots & \dots & \dots \\ 0 & 0 & 0 & \dots & 1 \end{pmatrix} \begin{pmatrix} I_0 \\ I_1 \\ I_2 \\ .. \\ I_{N+1} \end{pmatrix} = \begin{pmatrix} I_{in} \\ 0 \\ 0 \\ .. \\ I_{out} \end{pmatrix} \quad (20)$$

However, except if required by practical design, longitudinal currents coming out of either free end are ignored, thus it is necessary to consider only those free ends of the electrode where an existing current input is to be dissipated to the external environment. For an electrode with a single current injection point, $I_0 = I_{in}$, as in (20) but $I_{out} = 0$ in this case. As a final comment, if the injection point is located at any node junction between wire segments, e.g. segments n and n +1, this is equivalent to an injection point on the segment n +1 treated as an end segment and therefore rows are to be added similar to the first row of (20) with the value of the injected current on the right hand vector.

Since the electrode energization is caused by a current injected at a precise point and not by an electric field E_i, it holds that $E_i \cdot \Delta s = 0$, thus the vector components of the right hand in (20) almost all vanish. For other types of energization, as in the case of a receiving antenna, non-vanishing potential drops should be considered along the electrode due to the impressed field.

For an electrode composed of several interconnected wires forming a mesh, it is only necessary to consider the free ends of the structure. Some of them will be used to energize the structure while others will be terminal ends for which, with exceptions as noted above, the outgoing current will be zero. For each free end in the mesh, rows similar to the first and last of (20) have to be added, also accompanied by the corresponding value in the vector of the right hand.

Finally, the ground interface needs to be taken into account. It can be easily incorporated into the theoretical scheme by applying the theory of modified electrical images which adds to the calculations the contribution of image electrode with a weight factor F that for the modified image theory[16] and low frequency current energization is F=1. Thus, a final expression is obtained which is ready to be encoded on a computer,

$$\frac{1}{\sigma}[I_0(G(m,0)-G(m-1,0))-I_{N+1}(G(m,N)-G(m-1,N))]+$$
$$+\frac{1}{\sigma}\sum_{n=1}^{N} I_n(G(m,n)-G(m-1,n)-G(m,n-1)-G(m-1,n-1))+$$
$$+\frac{F}{\sigma}[I_0(G(m,0_I)-G(m-1,0_I))-I_{N+1}(G(m,N_I)-G(m-1,N_I))]+ \quad (21)$$
$$+\frac{F}{\sigma}\sum_{n=1}^{N} I_n(G(m,n_I)-G(m-1,n_I)-G(m,(n-1)_I)-G(m-1,(n-1)_I))=$$
$$=E_i(s_m)\cdot\Delta s.$$

The subscript source points I in the last terms of (21) refer to the image electrode source segments. Longitudinal currents on the image electrode have the same value as the corresponding currents on the real electrode, those being the mirror image of these.

The expression (21) is used to find the longitudinal currents in the electrode axis that make it equipotential. Once knowing the result, the absolute potential at any point in space and specifically in the ground surface, can be calculated. The absolute potential can be calculated from (7). Performing an integration by parts as in (10), the potential is

$$\phi(\vec{r}) = \int_{L'} \frac{-\vec{\nabla}'\vec{J}_s(\vec{r}'(s'))}{4\pi\sigma}\cdot\frac{ds'}{|\vec{r}-\vec{r}'(s')|} = -\frac{1}{\sigma}\int_{L'}\frac{\partial I(s')}{\partial s'}G(\vec{r},s')ds' =$$
$$=-\frac{1}{\sigma}\int_{L'}[\frac{\partial}{\partial s'}(I(s')G(\vec{r},s'))-I(s')\frac{\partial}{\partial s'}G(\vec{r},s')]ds' = -\frac{1}{\sigma}Cont(\vec{r})+ \quad (22)$$
$$+\frac{1}{\sigma}\int_{L'} I(s')\frac{\partial}{\partial s'}G(\vec{r},s')ds'$$

which, after applying the method of moments, results,

$$\phi(\vec{r}) = \frac{1}{\sigma}(I_0 G(\vec{r},0) - I_{N+1} G(\vec{r},N)) + \frac{1}{\sigma}\sum_{n=1}^{N} I_n (G(\vec{r},n) - G(\vec{r},n-1)) + \quad (23)$$
$$+ \frac{F}{\sigma}(I_0 G(\vec{r},0_I) - I_{N+1} G(\vec{r},N_I)) + \frac{F}{\sigma}\sum_{n=1}^{N} I_n (G(\vec{r},n_I) - G(\vec{r},(n-1)_I))$$

where, as in (21), the subscript I in the last term, stands for image segments source points which are affected by the factor F previously defined. This expression, can also be written in a more compact way as,

$$\phi(\vec{r}) = \frac{1}{\sigma}\sum_{n=0}^{N+1}(I_{n+1} - I_n) G(\vec{r},n) + \frac{F}{\sigma}\sum_{n=0}^{N+1}(I_{n+1} - I_n) G(\vec{r},n_I) \quad (24)$$

which reminds of the CSM approach by leakage currents to ground, which are obtained here by differencing the currents between adjacent segments. Note that there are N+2 longitudinal currents, if the end currents I_0 and I_{N+1} are included, and therefore N+1 leakage currents can be obtained.

The expression (23) will be used in this paper to calculate the grounding potential V_{PAT} and with the result, the grounding resistance $R_{PAT} = V_{PAT}/I_0$ is calculated. Grounding potential is defined as an average of the calculated potential by (23), for a broad set of points at the surface of the electrode. Such points are as previously described s_m points at the electrode surface.

IV. APLICATION EXAMPLES AND COMPARISON BETWEEN THE DIFFERENT METHODS

The figures below show the results for the potential profile on the ground for two different geometric configurations of conducting wires.

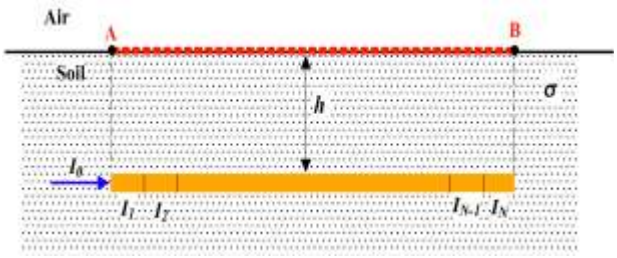

Fig 3. A conductive straight thin wire horizontally buried at depth h and powered by an incoming current I_0 at its left end. Some currents in the segments are also shown

The first one is a single electrode consisting of a straight rod of 2 m length, buried in the ground horizontally at 0.1 m depth from the surface and energized by a direct current of 10 A entering at its left end and moving to the right. It is assumed that the rod is a PEC and that the value for soil conductivity is of 100 Ωm (Fig. 3).

The second electrode is a regular mesh horizontally buried at 0.1 m depth and consists of 12 rods of 1 m length. A rod is added over one of the vertices of the mesh and placed vertically (Fig. 4). The 10A current injection point shows in Fig. 4. As in the previous example, it is assumed that the mesh is a PEC and that the same value for soil conductivity is used.

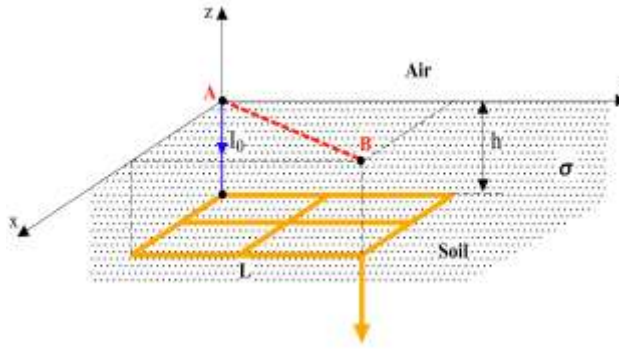

Fig 4. A conductive mesh composed of thin wires buried at depth h and powered by an incoming direct current I_0 through one corner. The soil is a single layered conducting medium of conductivity σ.

Figure 5 shows the potential profile at the ground surface along the electrode 1, on the line connecting points A and B as shown in Fig. 3. The results for the three methods are shown in the same Fig. 3. It is noted that the LCM method gives very similar results as the CSM method, whereas there are neat differences with the ones of the APM method.

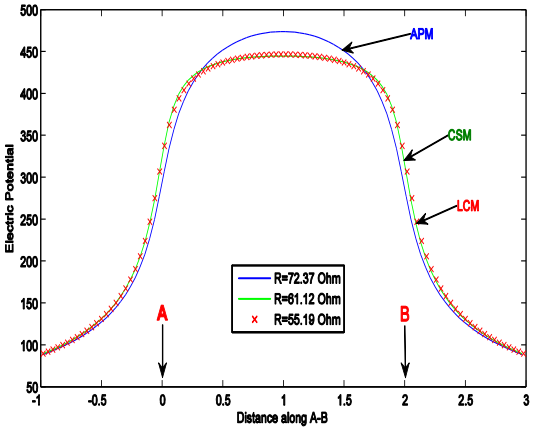

Fig 5. Electric potential profile along the line A-B on the ground above the buried rod from the electrode of Fig. 3. The results for the three methods used in the paper are shown. The solid black line stands for the APM method. The thin continuous line is the CSM method whereas the star dotted line corresponds to LCM method.

The same conclusions were obtained after analyzing the potential profile along the diagonal connecting points A and B on the soil surface above the conductive mesh of Fig. 4, as shown in Fig. 6. In both cases and for all methods used, the rods were divided into N = 30 segments each.

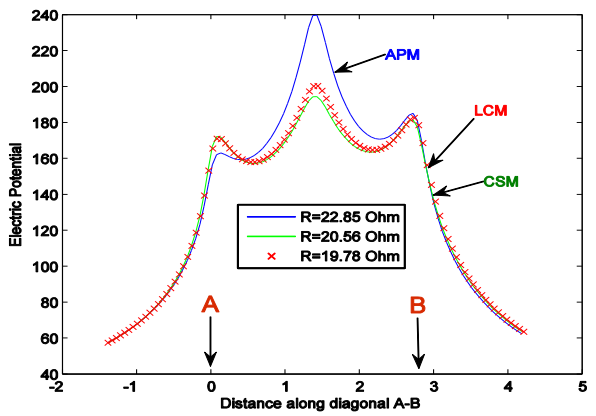

Fig 6. Electric potential profile along the diagonal A-B on the ground from the electrode of Fig. 4. It is easy to observe that over the mesh, along such a line A-B the step potentials achieved does not exceed 40 volts as can be seen from the curves.

In Fig. 5 and Fig. 6 the value of the grounding resistance R calculated by the three methods using the number of segments for each rod already mentioned is also shown.

TABLE I

GROUNDING RESISTANCE IN OHMS, ACCORDING TO THE **APM, CSM AND LCM** METHODS VERSUS THE NUMBER OF SEGMENTS **N** IN WHICH THE WIRES ARE DIVIDED.

	Electrode Fig. 3			*Electrode Fig. 4*		
N	**APM**	**CSM**	**LCM**	**APM**	**CSM**	**LCM**
30	72.370	61.120	55.190	22.850	20.560	19.780
50	65.616	61.039	58.130	21.820	20.556	20.173
70	63.481	60.995	59.491	21.495	20.554	20.361
90	62.636	60.965	60.150	21.367	20.553	20.454
110	62.264	60.944	60.473	21.311	20.552	20.499
130	62.091	60.927	60.633	21.285	20.551	20.523
200	61.942	60.887	60.778	21.264	20.549	20.542
300	61.929	60.853	60.787	21.263	20.547	20.544
400	61.930	60.830	60.780	21.264	20.546	20.543

Table I shows the values of the grounding resistance of the electrodes in Fig. 3 and Fig. 4 which are obtained by applying the three methods when the wires of the electrodes are divided into a number N of segments. Regarding the APM method, it is possible to analytically calculate the value of the grounding resistance, at least for the electrode of Fig. 3, from the expression

$$R_{PAT} = \frac{1}{L}\int_{-L/2}^{L/2} V(z)dz$$

$$V(z) = \frac{\rho}{4\pi L}\left\{\log\left[\frac{z+L/2+\sqrt{(r)^2+(z+L/2)^2}}{z-L/2+\sqrt{(r)^2+(z-L/2)^2}}\right]+\log\left[\frac{z+L/2+\sqrt{(2h+r)^2+(z+L/2)^2}}{z-L/2+\sqrt{(2h+r)^2+(z-L/2)^2}}\right]\right\}$$

where the variable z stands for a coordinate along the wire axis with the origin located at the center, r is the radius of the wire and L its length. Note that the average in the electric potential over the conductor surface has been calculated because in the APM method the electrode itself is not equipotential. With the values of L and ρ defined above, a value of 61.73 Ohm is obtained for the grounding resistance, which differs by 0.3% from the asymptotic value of 61.93 Ohm given by the APM method. The reason for this discrepancy is to be found in the APM method itself used here. Each segment of the wire is replaced by a point source of leakage current. As the partition is refined, the result is closer to the exact value. The same applies to the CSM method in which each segment is also replaced by a point source of leakage current but this time non-constant along the wire axis. This results in a slow convergence to the asymptotic value as the partition is refined. The LCM method provides a fast convergence to the asymptotic value of the grounding resistance as shown in Table I.

The dependence of grounding resistance with the number of segments of the wires is shown in Fig. 7 calculated by using the three methods. It is observed that the LCM method and the CSM method, as was pointed out earlier, clearly converge to a common asymptotic value.

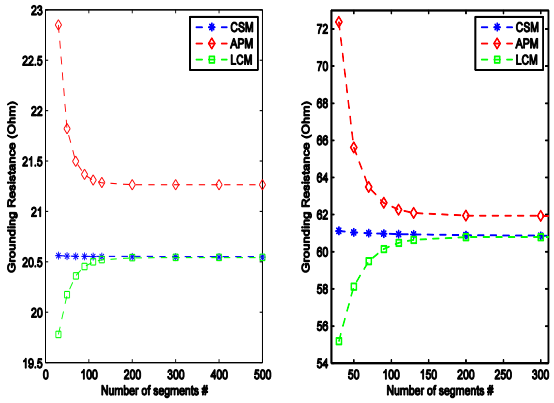

Fig 7. Grounding resistance versus the number of segments in which each rod of the structure is divided when calculated by using the three methods APM, CSM and LCM. The results for electrode of Fig. 3 are shown in the right hand, whereas on the left hand it is shown the results for electrode of Fig. 4.

It can be stated that the LCM method gives a lower bound to the grounding resistance whilst the CSM method gives an upper bound of it. It can also be seen that the APM method slightly deviates from that behavior (by 0.16% approximately for the single electrode) and the potential profile supplied is significantly different, especially in the central area, from those obtained by the two other methods.

The reported behavior in the calculation of the grounding resistance by the two methods LCM and CSM, suggests the possibility of assigning an error value to grounding resistance calculation. It may be taken as the interval radius of the grounding resistance obtained by both of the methods. As the representative value of the resistance, it can be taken as the average value of the grounding resistance obtained also by both of the methods. The results of such a procedure in terms of absolute error value and percentage over the representative value of the grounding resistance are shown in Table II.

TABLE II
ESTIMATED ERROR IN GROUNDING RESISTANCE CALCULATIONS VERSUS THE NUMBER OF SEGMENTS **N** IN WHICH THE WIRES ARE DIVIDED.

	Fig. 3		*Fig. 4*	
N	**±Err**	**%**	**±Err**	**%**
30	2.965	5.4	0.39	2.0
50	1.455	2.5	0.192	1.0
70	0.752	1.7	0.097	0.5
90	0.408	0.7	0.050	0.3
110	0.234	0.4	0.027	0.2
130	0.147	0.3	0.014	0.07
200	0.055	0.09	0.004	0.02

V. CONCLUSIONS

In this paper we have implemented numerical codes for three methods in order to calculate the grounding resistance and potential profile at ground level produced by two examples of thin-wire structures powered by low frequency current. In the LCM method, starting from a set of currents along the wires, which are part of the buried structure, they are taken as sources of electromagnetic fields on the soil. Solving Maxwell equations numerically by using the method of moments, a solution that provides the value of the grounding resistance and the potential profile in the soil is obtained which is applied to the configurations of wires. In parallel, a more usual scheme based on leakage currents, the CSM, has been coded and used to analyze the same configurations. A comparison of the results obtained by applying the CSM and LCM methods to the same configurations of wires has been made. A third method, the APM, has also served for comparison.There has been found a good agreement between the LCM and the CSM method and greater discrepancy with the APM method. Both, the LCM and the CSM methods show a tendency towards a common asymptotic value of the grounding resistance when the segmentation applied to the wires is refined, the LCM method supplying a lower bound to the grounding resistance. This property was used to estimate the error in the determination of the grounding resistance when any of the above methods is used according with a precise wire segmentation.

ACKNOWLEDGMENTS

The authors would like to thank the Departments of Electrical Engineering, Applied Mathematics and Applied Physics of the *Escuela Técnica Superior de Ingeniería y Diseño Industrial* (ETSIDI) at Polytechnical University of Madrid (UPM) for their support to the undertaking of the research summarized here. Furthermore, the authors appreciate the useful suggestions and selfless assistance of Prof. P. Navarro. Finally, the authors would like to thank Ms. Gabriela Andres for her contribution to the linguistic correction of the original paper.

REFERENCES

[1] R. J. Heppe. "Computation of Potential at Surface Above an Energized Grid or other Electrode, Allowing for Non-Uniform Current Distribution". IEEE Transactions on Power Apparatus and Systems, Vol. PAS-98, No.6, pp. 1978 – 1989, 1979.

[2] D. L. Garrett, J. G. Pruitt. "Problems Encountered With The Average Potential Method of Analyzing Substation Grounding Systems". IEEE Transactions on Power Apparatus and Systems, Vol. PAS-104, No. 12, pp. 3585 - 3596, 1985.

[3] R. P. Nagar, R. Velazquez, M. Loeloeian, D. Mukhedkar, Y. Gervdis. "Review of Analytical Methods for calculating the Performance of Large Grounding Electrodes. Part I: Theoretical Considerations". IEEE Transactions on Power Apparatus and Systems, Vol. PAS-104, No. 11, pp. 3123 - 3133, 1985.

[4] M. Loeloeiaam, R. Velazquez, D. Mukhedkar. "Review of Analytical Methods for calculating the Performance of Large Grounding Electrodes. Part II: Numerical Results". IEEE Transactions on Power Apparatus and Systems, Vol. PAS-104, No. 11, pp. 3134 – 3141, 1985.

[5] J. Nahman and D. Salamon. "Earthing system modelling by element aggregation". *IEE proceedings C, Vol. 133, No. I, pp 54-58, 1986.*

[6] N. H. Malik. **"**A Review of the Charge Simulation Method and its Applications". IEEE Transactions on Electrical Insulation Vol. *24 No. 1, pp. 3-20, 1989.*

[7] A. P. Sakis Meliopoulos, Feng Xia, E. B. Joy, G. J. Cokkinide. "An advanced Computer Model for Grounding System Analysis. IEEE Transactions on Power Delivery, Vol. 8, No. 1,pp. 13 – 23, 1993.

[8] J.G. Sverak. "Progress in Step and Touch voltage equations of ANSY/IEEE Std 80 Historical Perspective". IEEE Transactions on Power Delivery, Vol. 13, No. *3, pp.* 762 – 767, 1998.

[9] E. Bendito, A. Carmona, A. M. Encinas, and M. J. Jiménez. "The Extremal Charges Method in Grounding Grid Design". IEEE Transactions on Power Delivery, Vol. 19, No. 1, pp. 118-123, 2004.

[10] F. P. Dawalibi, J. Ma and R. D. Southey: "Behaviour of Grounding Systems in Multylayer Soils: A Parametric Analysis", IEEE Transactions on Power Delivery, Vol. 9, No. 1, pp. 334-342, 1994.

[11] S. Vujević and M. Kurtović: "Numerical Analysis of Earthing Grids Buried in Horizontally Stratified Multilayer Earth", International Journal for Numerical Methods in Engineering, Vol. 41, No. 7, pp. 1297-1319, 1998.

[12] R. F. Harrington: "Field Computation by Moment Methods", IEEE Press, New York, 1993.

[13] Y. L. Chow, M.M. Elsherbiny, M.M.A.Salama. "Efficient computation of rodbed grounding resistance in a homogeneous earth by Galerkin's moment method". *IEE Proc.-Gener. Trunsm. Distrib., Vol. 142, No. 6, November 1995.*

[14] S. Berberovic, Z. Haznadar, Z. Stih. "Method of moments in analysis of grounding systems". Engineering Analysis with Boundary Elements, Vol. 27, pp. 351–360, 2003.

[15] Z.-X. Li and J.-B. Fan: "Numerical Calculation of Grounding System in Low-Frequency Domain Based on the Boundary Element Method", International Journal for Numerical Methods in Engineering, Vol. 73, No. 5, pp. 685-705, 2008.

[16] L.D. Grcev, "Computer analysis of transient voltages in large grounding systems," *IEEE Transactions on Power Delivery*, Vol.11, No.2, pp.815-823, 1996.

[17] L. Grcev, F. Dawalibi, "An electromagnetic model for transients in grounding systems,'' IEEE Transactions on Power Delivery, vol. 5, no. 4, pp. 1773-1781, October 1990.

[18] IEEE Guide for Safety in AC Substation Grounding, IEEE Std. 80-2000, May 2000.

BIOGRAPHIES

E. Faleiro was born in Madrid, Spain. He received the B.S. degree in Theoretical Physics from the *Universidad Complutense de Madrid* (UCM), in 1982 and the Ph.D. degree in Fundamental Physics from the UCM. in 1998.

From 1990 to 1993, he was an Assistant Professor with the Applied Physics Department at the Polytechnic University of Madrid (UPM). Since 1994, he has been a Full Professor with the Applied Physics Department of the *Escuela Técnica Superior de Ingeniería y Diseño Industrial* (ETSIDI) at UPM. He is the author of more than 20 articles in the area of theoretical and experimental physics in journals of JCR. His research interests include cosmic rays, fractals, quantum chaos, biomedical time series analysis and, more recently, grounding grid analysis. E-mail: eduardo.faleiro@upm.es

G. Asensio was born in Madrid, Spain. He received the B.S. degree in Theoretical Physics from the *Universidad Complutense of Madrid* (UCM), in

1987 and the Ph. D. degree in Applied Mathematics from the Polytechnic University of Madrid (UPM) in 2002.

From 1987 to 2003, he was a Professor with the Applied Mathematics Department at UPM. Since 2003, he has been a Full Professor with the Applied Mathematics Department of the *Escuela Técnica Superior de Ingeniería y Diseño industrial* (ETSIDI) at the UPM. Since 2002, he has been a member of Applied Bioengineering Research Group at UPM. His research interests include computational math and programming applied to magnetic measurements and grounding grid analysis. E-mail: gabriel.asensio@upm.es

D. García was born in Madrid, Spain. He received the B.S degree in Industrial Engineering from the *Universidad Carlos III* of Madrid, in 2003. Since 2003 he is a Associated Professor with the Electrical Engineering Department of the *Escuela Técnica Superior de Ingeniería y Diseño Industrial* (ETSIDI) at the Polytechnic University of Madrid (UPM). He is currently pursuing a Ph. D. degree in the area of electrical power transmission.

Since 2000 he has been working in FEMAB engineering, making projects up to 400kV of power lines. His research interests include grounding grid analysis, overvoltages in shield of underground cable and tower spotting of overhead lines. E-mail: daniel.gpuertas@upm.es

G. Denche was born in Madrid, Spain, in 1976. He received the B.S degree in Industrial Engineering from the Polytechnic University of Madrid (UPM), in 2002. Since 2006 he has been an Associated Professor with the Electrical Engineering Department of UPM. He is currently pursuing a Ph. D. degree in the area of electrical power transmission.

Since 2003, he has been working at *RED ELECTRICA DE ESPAÑA, TSO* (Transmission System Operator) of the Spanish Electricity System where he is a senior engineer at the Engineering Lines Department. His research interests include grounding grid analysis and overvoltage in metallic screen of underground cable. E-mail: gdenche@ree.es

J. Moreno was born in Yepes (Toledo), Spain. He received the B.S degree in Industrial Engineering from the Polytechnic University of Madrid (UPM), in 1989 and the Ph. D. degree in Industrial Engineering, in 1995.

From 1989 to 1995, he was a Professor with the Electrical Engineering Department at UPM. Since 1995, he has been a Full Professor with the Electrical Engineering Department of the *Escuela Técnica Superior de Ingeniería y Diseño Industrial* (ETSIDI) at UPM. Since 1995, he has been Director of the Magnetics Measurements Laboratory at UPM. He is an expert referee of projects for the Accreditation Agency for Research, Development and Technological Innovation (AIDIT). His research interests include magnetic measurements and grounding grid analysis. E-mail: jorge.moreno@upm.es